Carbohydrate Polymers 332 (2024) 121877

Contents lists available at ScienceDirect

Carbohydrate Polymers

journal homepage: www.elsevier.com/locate/carbpol

Processing factors affecting roughness, optical and mechanical properties of nanocellulose films for optoelectronics

Joice Jaqueline Kaschuk [a,b], Yazan Al Haj [c], Joaquin Valdez Garcia [d], Aleksi Kamppinen [d], Orlando J. Rojas [a,b], Tiffany Abitbol [e,f], Kati Miettunen [d], Jaana Vapaavuori [c,*]

[a] Department of Bioproducts and Biosystems, School of Chemical Engineering, Aalto University, FI-00076, Aalto, Espoo, Finland
[b] Department of Chemical and Biological Engineering, 2360 East Mall, The University of British Columbia, V6T 1Z3 Vancouver, BC, Canada
[c] Department of Chemistry and Materials Science, School of Chemical Engineering, Aalto University, FI-00076 Aalto, Finland
[d] Department of Mechanical and Materials Engineering, Faculty of Technology, University of Turku, FI-20500 Turku, Finland
[e] RISE Research Institutes of Sweden, SE-114 28 Stockholm, Sweden
[f] Institute of Materials, School of Engineering, EPFL, Station 12, 1015 Lausanne, Switzerland

ARTICLE INFO

Keywords:
Optoelectronic
Solar cells
Biobased substrates
Light management
Sustainable electronics

ABSTRACT

This work aims to understand how nanocellulose (NC) processing can modify the key characteristics of NC films to align with the main requirements for high-performance optoelectronics. The performance of these devices relies heavily on the light transmittance of the substrate, which serves as a mechanical support and optimizes light interactions with the photoactive component. Critical variables that determine the optical and mechanical properties of the films include the morphology of cellulose nanofibrils (CNF), as well as the concentration and turbidity of the respective aqueous suspensions. This study demonstrates that achieving high transparency was possible by reducing the grammage and adjusting the drying temperature through hot pressing. Furthermore, the use of modified CNF, specifically carboxylated CNF, resulted in more transparent films due to a higher nanosized fraction and lower turbidity. The mechanical properties of the films depended on their structure, homogeneity (spatial uniformity of local grammage), and electrokinetic factors, such as the presence of electrostatic charges on CNF. Additionally, we investigated the angle-dependent transmittance of the CNF films, since solar devices usually operate under indirect light. This work demonstrates the importance of a systematic approach to the optimization of cellulose films, providing valuable insight into the optoelectronic field.

1. Introduction

The fast growth of the optoelectronics industry has triggered an urgent need for sustainable materials to mitigate the environmental impact of their disposal (Liu et al., 2022). Nanocellulose (NC), a versatile nanomaterial derived from the most abundant biopolymer on Earth (cellulose), responds to this challenge as a standout candidate characterized by its environmental sustainability (Chen et al., 2021; Dufresne, 2013). By definition, NC presents at least one dimension of 100 nm or less, and the most common NC include cellulose nanocrystal (CNC, 100–200 nm in length and 10–30 nm in diameter), and cellulose nanofibril (CNF, with an average diameter of 2–50 nm and length of 1–15 μm) (Lengowski et al., 2023; Solhi et al., 2023). NC from diverse sources has been extensively studied especially regarding cellulose processing techniques—whether physical, chemical, or biological — to yield CNC and CNF (Deepa et al., 2015; Hancock et al., 2023; Haron et al., 2021; Pires et al., 2019; Pradhan et al., 2022; Rol et al., 2020; Squinca et al., 2020; Yang et al., 2023). These studies share a common overarching aim: to elucidate the capability of varied cellulose sources in generating NC characterized by distinct dimensions, surface charges, and dispersion.

Engineered into film form, CNF exhibit enhanced mechanical and optical properties due to their high aspect ratio and the potential for functionalization. These films have attracted considerable attention as they combine inherent renewability and biodegradability with impressive mechanical strength and optical transparency (Ahankari et al., 2021; Kaschuk et al., 2021), making them highly suitable for optoelectronic applications that demand both transparency and mechanical endurance.

The mechanical strength of NC films is critical for optoelectronics

* Corresponding author.
E-mail address: jaana.vapaavuori@aalto.fi (J. Vapaavuori).

https://doi.org/10.1016/j.carbpol.2024.121877
Received 27 July 2023; Received in revised form 24 January 2024; Accepted 25 January 2024
Available online 2 February 2024

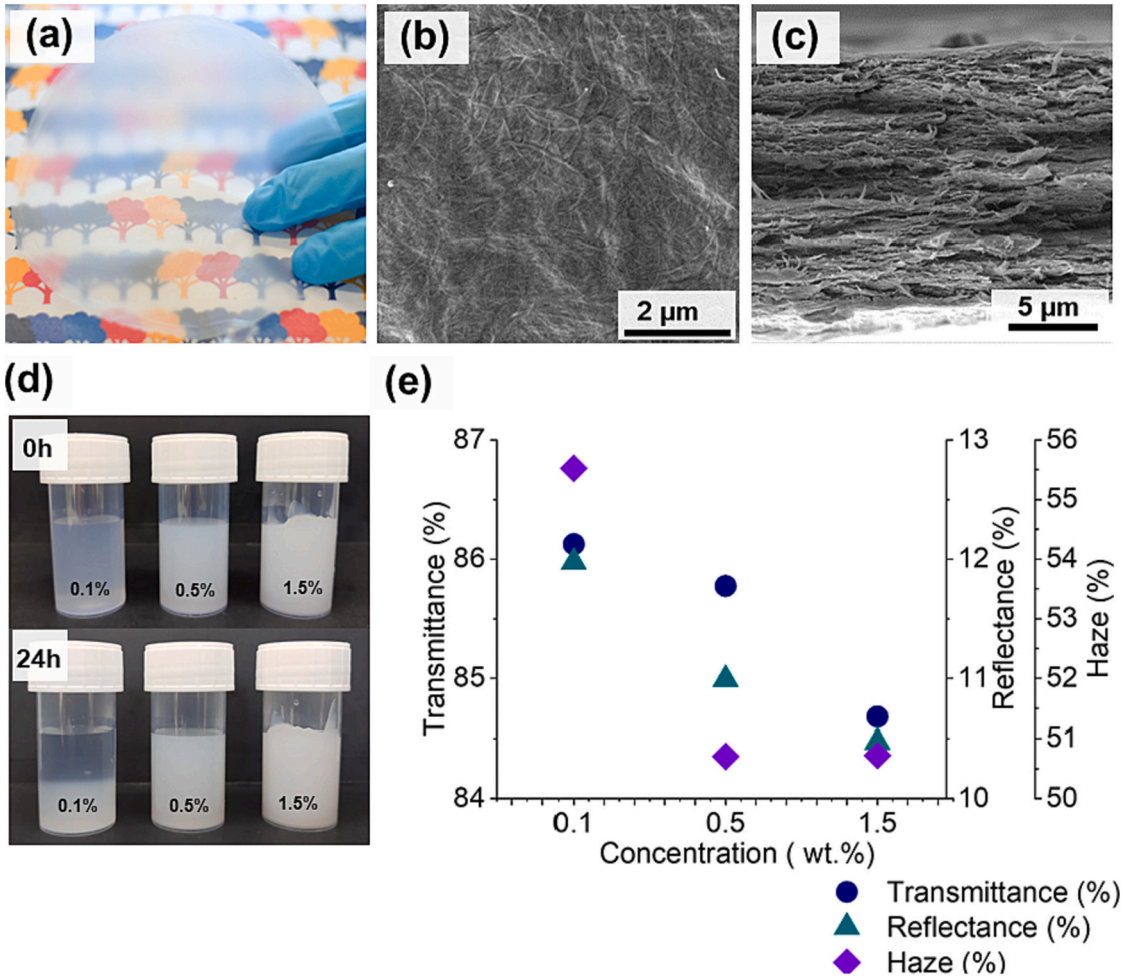

Fig. 1. (a) Photograph, (b) SEM surface image, and (c) SEM cross-section image of a film produced with a concentration of 0.5 % CNF. (d) CNF suspensions with different concentrations and their stability behavior after 24 h. (e) Optical properties at 550 nm for CNF films produced by different concentrations (0.1, 0.5, and 1.5 wt%).

durability and functional longevity (Chattopadhyay & Labram, 2022). Recent literature underscores the remarkable mechanical characteristics of various NC grades. Decolorized lignocellulosic nano paper, for instance, has been demonstrated to possess an ultimate tensile strength of approximately 105 MPa, suggesting its suitability for photovoltaic applications (Jiang et al., 2020). Similarly, TEMPO CNF has exhibited considerable mechanical resilience, with an ultimate tensile strength near 93 MPa, reinforcing its potential for robust electronic components (Chen et al., 2018). Moreover, the mechanical properties of TEMPO CNF/Ag NWs composite, with an ultimate tensile strength of 70.1 MPa, reveal its applicability in organic solar cells (Lin et al., 2021).

Optical properties, such as transparency, translucency, brightness, and antireflection, are influenced by multiple variables, including CNF orientation, aspect ratio, nanofibril morphology, and drying procedure (Fukuzumi et al., 2009; Kaschuk et al., 2022; Koga & Nogi, 2015; Podsiadlo et al., 2007; Qing et al., 2015; Yang et al., 2022). By changing these variables, it is possible to manipulate the light interaction that occurs at the fibril interface (surface) and consequently the performance of optoelectronic substrates (Jacucci et al., 2020; Koga & Nogi, 2015; Zhang et al., 2018; Zhu et al., 2014). For instance, applications such as solar cells can derive benefits from the interactions of light with NC films, making them applicable for light management (Jia et al., 2017). Generally, the combination of high transparency, high haze, and antireflection properties can enhance the amount of light absorbed by the solar cells, thereby positively impacting their power conversion efficiency (Fang et al., 2014; Jia et al., 2017).

Lastly, NC films lack conductivity, an essential characteristic in electronic devices (Wang & Huang, 2021). As a result, it is necessary to apply a conductive layer on these materials, the quality of which depends on the films' surface roughness. Higher surface roughness may cause an uneven conductive layer, leading to short circuits or decreased conductivity (Bragaglia et al., 2019). This feature is quite challenging to achieve. Once NC films are obtained by the collapse and entanglement of fibers, roughness in μm scale is usually obtained (Shanmugam et al., 2020).

While NC films have been extensively researched (Fukuzumi et al., 2009; Kim et al., 2021; Qing et al., 2015; Yang et al., 2018; Zhao et al., 2017), there is still a gap in the scientific literature when it comes to systematically and specifically exploring how small processing changes, such as concentration and composition of suspensions, grammage, and drying temperature impact produced films' roughness, and mechanical and optical properties considering the basic requirements for optoelectronics. Herein, the central hypothesis is that small adjustments to the processing factors of CNF films can produce a substrate for higher-performance optoelectronic.

Although our findings show that variations in roughness, and optical and mechanical properties are induced by straightforward changes in processing, such as suspension concentration/stability, drying temperature, and NC grades, these substrates must still be submitted for further alterations before being employed in optoelectronics. While the films created here had adequate mechanical qualities, their high surface roughness would need to be further smoothened to facilitate the

Table 1
Nanocelluloses (NC) with the respective suspension concentration (Conc), grammage (Gramm), and temperature (Temp) used the produce films with different thicknesses, densities, and roughness and its respective transmittance (T), reflectance (R), and haze at 550 nm. Here, the side of the film that comes into contact with the membrane during the filtration process is referred to as the Bottom, while the side that eventually comes into contact with air is referred to as the Top.

NC	Conc (wt%)	Gramm ($g{\cdot}m^{-2}$)	Temp. (C)	Thickness (μm)	Density ($g{\cdot}cm^{-3}$)	Tensile strength (MPa)	Roughness bottom side (μm)	Roughness top side (μm)	T (%)	R (%)	Haze (%)
CNF	0.1	30	30	23 ± 1.0	1.12 ± 0.03	237 ± 5	1.5 ± 0.2	1.3 ± 0.2	86.1	12.0	55.5
	0.5			26 ± 3	1.07 ± 0.02	192 ± 11	0.5 ± 0.1	0.6 ± 0.1	85.8	11.0	50.7
	1.5			33 ± 5	1.05 ± 0.05	153 ± 15	0.7 ± 0.04	1.0 ± 0.2	84.7	10.5	50.7
	0.5		90	18 ± 1	1.25 ± 0.02	233 ± 5	0.3 ± 0.04	0.5 ± 0.04	82.4	17.8	55.1
		60	30	47 ± 2	1.11 ± 0.02	196 ± 5	1.5 ± 0.1	2.0 ± 0.2	84.0	12.5	50.4
Enz-CNF				43 ± 2	1.09 ± 0.10	133 ± 4	1.4 ± 0.2	1.0 ± 0.1	82.8	14.4	71.9
CMC-CNF				54 ± 1	0.95 ± 0.02	173 ± 8	2.7 ± 0.7	1.0 ± 0.1	86.1	10.9	66.7
TOCNF				47 ± 2	1.3 ± 0.05	188 ± 6	1.2 ± 0.2	0.8 ± 0.1	85.6	10.7	50.4

deposition of an even conductive layer. Also, to optimize the films for the targeted application, their high reflectance at high incidence angles of incoming light, along with their total transparency, should still be improved. However, assembled all together, our results form a systematic summary of processing parameters that affect the performance of NC films for optoelectronics.

2. Materials and methods

2.1. NC specifications

Cellulose nanofibril suspensions (CNF) were produced from a never dried, fully bleached, and fines-free sulphite birch pulp (Kappa number = 1, and DP = 4700), which was disintegrated (six passes) through a high-pressure fluidizer (pressure of 1500 bars, Microfluidics M110P, Microfluidics Int. Co., Newton, MA) (Ajdary et al., 2019).

TEMPO-oxidized cellulose nanofiber suspensions (TOCNF) were produced from never-dried birch fibers by TEMPO-mediated oxidation (2,2,6,6-tetramethylpiperidine-1-oxyl) (Saito et al., 2007), and fibrillated (one pass) using a high-pressure fluidizer (pressure of 1500 bars, Microfluidics M110P, Microfluidics Int. Co., Newton, MA).

Enzymatic cellulose nanofibril suspensions (ENZ-CNF) were obtained from a commercial never-dried, totally chlorine-free bleached softwood sulphite dissolving pulp (Domsjö Fabriker AB, Sweden). First, the pulp was submitted to an enzymatic pre-treatment, followed by miocrofluidization comprised of 3 passes at 400 bar and 5 additional passes at 1700 bar (Microfluidics Corp., United States).

Carboxymethylated cellulose nanofibril suspensions (CMC-CNF) were also obtained from a commercial never-dried, totally chlorine-free bleached softwood sulphite dissolving pulp (Domsjö Fabriker AB, Sweden). After carboxymethylation pre-treatment, the fibers were passed 1 time at 1700 bar through a high-pressure homogenizer (Microfluidizer M-110EH, Microfluidics Corp., United States).

2.2. NC film preparation

Homogeneous and translucent NC films were produced by air pressure filtration followed by hot pressing (Fig. 1 - a). This methodology presents a few advantages compared to casting since the procedure happens in a shorter time and the inner structure of the films can be modified by how fast the water is removed from its wet form. Even though the methodology used here presents a huge difference in practice (Benítez & Walther, 2017), through the formation of the film the changes observed in the colloidal suspension properties are very similar to those observed in the casting.

The stock NC suspensions (Table S1) were diluted until the desired concentration and stirred overnight. The bubbles from the suspensions were removed by reduced pressure using a vacuum oven at room temperature.

An air pressure filtration equipment integrated by a tripod chamber (inner diameter of 12 cm, height 8.5 cm) was used to produce a wet film. The wet films were produced on the top of a polyvinylidene fluoride (PVDF) membrane filter (0.45 μm pore size, hydrophilic PVDF, 142 mm membrane, Dupore), that was placed on the top of Sefar Nitex polyamine monofilament fabric mesh. The used air pressure was 1.0 bar, and the filtration was performed until all the water was removed from the suspension.

Lastly, the wet film and the membranes were put as a sandwich with the following configuration: metal sheet, five layers of regular filter paper, Sefar Nitex mesh, PVDF membrane, wet film, Sefar Nitex mesh, five layers of regular filter paper, and metal sheet. Finally, the sandwich was hot pressed in a Carver Laboratory Press 18200-213 made by Fred S. Carver, Inc. Hydraulic Equipment (Summit, NJ, U.S.A.) for 1 h. A total of eight films were created (as shown in Table 1). These films were produced by varying three key parameters: the concentration (0.1, 0.5, and 1.5 wt%), the grammage (30 $g{\cdot}m^{-2}$ and 60 $g{\cdot}m^{-2}$), the pressing temperature (30 °C and 90 °C), and NC grades.

2.3. Characterizations

The turbidity of the NC suspensions was evaluated using a Hach Turbidimeter. The NC suspensions were diluted to 0.05, 0.1, and 0.2 wt %, and the turbidity in NTU units was measured for each suspension together with the exact concentration of each suspension gravimetrically. The given turbidity value is reported at 0.1 wt% based on interpolation from the linear regression of the concentration series.

To determine the nano fraction, 0.02 wt% NC suspensions were centrifuged at high speed (1000*g*; 15 min). Then, the solid content of the supernatant was measured, indicating the colloidally stable fraction. The ratio in mass% of the solids recovered from the supernatant relative to the total dry mass of the initial suspension gives the nano fraction. All solid contents are measured gravimetrically.

Thicknesses of NC films were measured using an L&W Micrometer (Lorentzen & Wettre Products, ABB, Switzerland), which in turn were used to calculate the volume of 1 cm^2 samples and their densities (relation between the weight by the volume) (Chen et al., 2020). The average thicknesses were obtained from the measurements of 20 different areas within the film.

Roughness-RA stylus profilometer (DektakXT®, Bruker) with a diamond tip was used to measure film roughness. Roughness results are an average of five topographic line scans, using the following parameters: 2 μm tip radius, 65.5 μm measurement range, 100 μm measurement length, 1 mg Stylus force, 30 s measurement duration, 0.37 μm/pt. resolution, and hills and valleys profile type. The graphics were plotted using arithmetic average roughness values.

Mechanical properties – For tensile testing, strips (45 mm long; 6 mm wide) were cut from each film, with the average grammage determined from the average mass of four strips. Stress-strain curves were measured using an MTS 3125 tensile tester with a strain rate of 5 mm min^{-1}, with films equilibrated for several days before testing at standard conditions

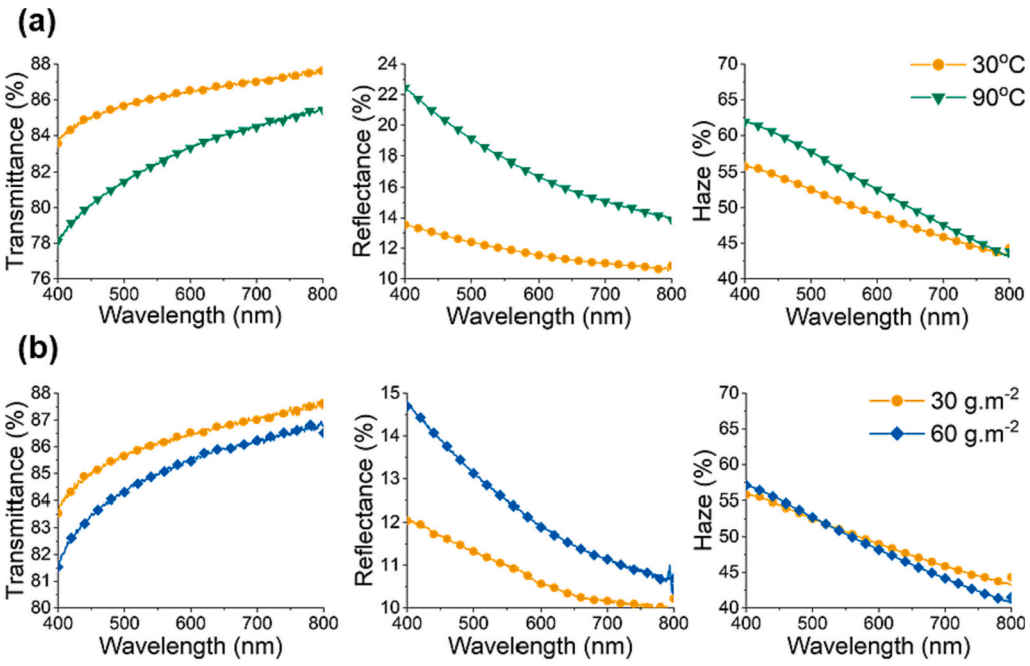

Fig. 2. Optical properties of CNF films. (a) Influence of the temperature during the hot press and (b) Influence of the grammage.

(23 °C and 50 % relative humidity).

The top and cross-sectional morphologies of the obtained CNF films were observed using scanning electron microscopy (SEM, Tescan MIRA 3) with an acceleration voltage of 5.0 kV. Before imaging, the CNF samples were coated with a thin layer of gold-palladium (Au-Pd, 80-20) using a Q150T coater (Quorum) to enhance their conductivity and prevent charging.

The optical properties (transmittance, haze, and reflectance) from 400 nm to 800 nm (transmittance, haze, and reflectance) with direct illumination were obtained using the Diffuse Reflectance Accessory coupled to UV–Vis-NIR Agilent Cary 5000 both from Agilent Technologies.

Angle-dependent transmittance to investigate antireflection properties was measured using a customized optical setup. A Thorlabs SLS201L/M Stabilized Tungsten-Halogen Light Source was used as a white light source, then equipped with a Thorlabs SLS201C collimator and a pair of plano-convex lenses with focal lengths of 60- and 30-mm. Transmitted light was collected inside an Artifex Engineering 100 mm Integrating Sphere mounted on a Thorlabs KPRMTE/M motorized precision rotation stage. The light was transmitted from the integrating sphere to a Thorlabs CCS200/M compact Czerny-Turner spectrometer through an optic fiber. NC films were mounted on the light entrance of the integrating sphere and the film transmittance was measured with an integration time of 850 ms. Measurements were taken every 5° from 0° to 65° by rotating the integrating sphere. These measurements were then subtracted from a reference measurement without any obstruction at the entrance of the integrating sphere to obtain the transmittance spectra.

3. Results and discussion

The results of this study are structured into two major parts. The first part (3.1) focuses on the evaluation of films produced using a single NC grade (CNF). We investigate how various film properties change when altering the concentration (0.1, 0.5, and 1.5 wt%), grammage (30 g·m^{-2} and 60 g·m^{-2}), and pressing temperature (30 °C and 90 °C). In the second part (3.2), we broaden our scope to assess different NC grades, including CNF, TOCNF, ENZ-CNF, and CMC-CNF. These films were produced using suspensions with a consistent 0.5 wt% concentration, a grammage of 60 g·m^{-2}, and a temperature of 30 °C. A summary of the main results is presented in Table 1.

3.1. Impact of processing factors on single NC grade films

3.1.1. CNF film formation, roughness, and optical properties of films produced by different concentrations

It is commonly reported in the literature that several interactions govern the film formation, including fibril aggregations, entanglements, and electrostatic forces such as hydrogen bonds between hydroxyl groups (Benítez & Walther, 2017; Henriksson et al., 2008; Niinivaara & Cranston, 2020; Qing et al., 2015). All the films presented a translucent structure with a highly dense and laminar-packed material as observed by the photographs and SEM images (Figs. 1 – a, b, c, S1).

It was observed that the stability and the homogeneity of the initial suspensions also play an important role in film formation. A stable CNF suspension presents a strong hygroscopic character of cellulose, as well as a high aspect ratio and high specific surface area of the nanofibrils (Nechyporchuk et al., 2016). Herein, by changing the concentration of the suspensions, we observed differences in their stability. Once, after 24 h, a phase separation for lower concentration (0.1 wt%, Fig. 1-d) was observed. In higher concentrations, the intense network stabilization among the nanofibers occurs keeping the suspensions stable. As illustrated in Fig. 1 – d, CNF suspensions were stable between the concentrations 0.1 and 0.5 wt%.

After CNF films (same base weight) were manufactured, different optical properties were obtained (Figs. 1 – e, S2). For instance, the CNF suspension with the highest concentration (1.5 wt%) presented greater opacity and consequently, the film presented the lowest transparency, reflectance, and haze values. At the other end of the studied range, the CNF suspension with the lowest concentration (0.1 wt%) generated films with higher transparency, reflectance, and haze values. For all the cases, the explanation lays down on the inhomogeneous structure obtained by the flocculation within the suspensions before the film formation. The same explanation applies to the different values of thickness, density, and roughness of these films (Table 1), even if produced at the same basis weight (grammage).

In this study, the impact of suspension concentration on film roughness was also assessed. Higher concentrations of CNF suspensions

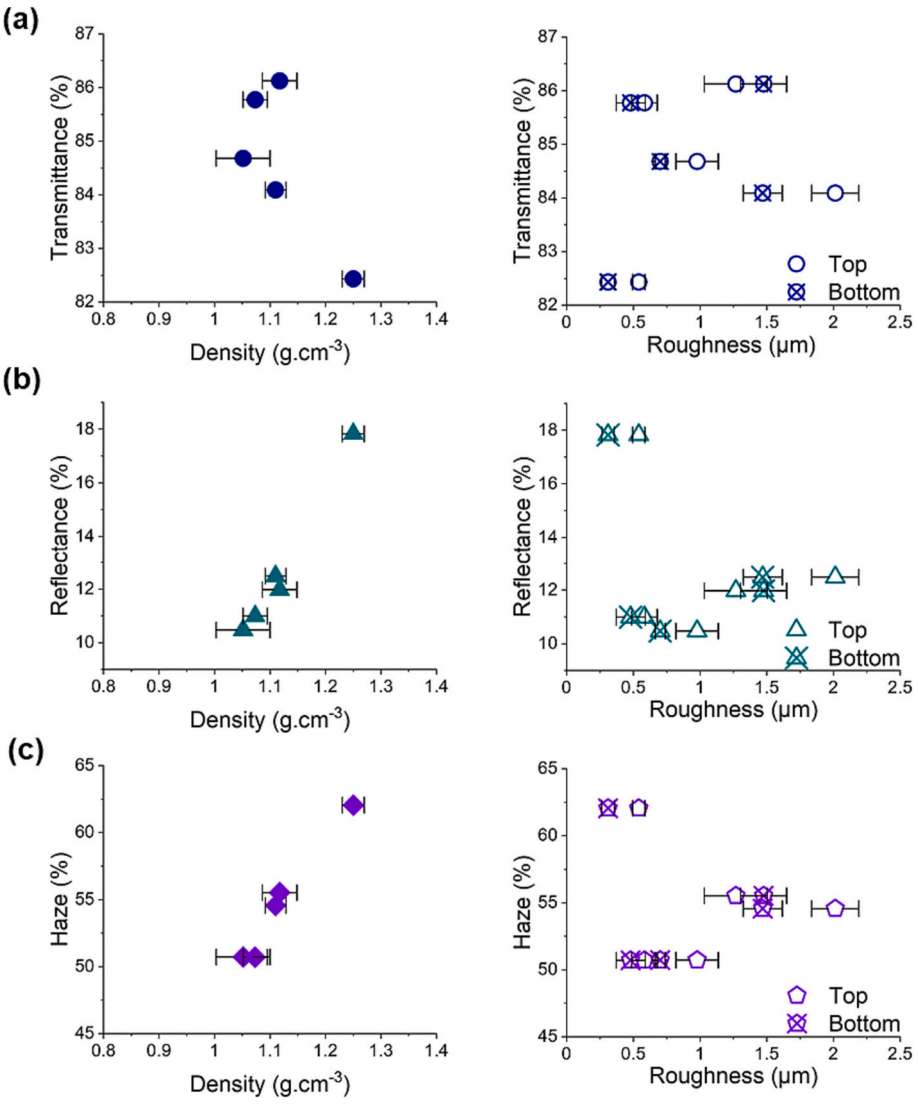

Fig. 3. Correlation among density and roughness of all CNF films with (a) transmittance, (b) reflectance, and (c) haze. Here, the side of the film that comes into contact with the membrane during the filtration process is referred to as Bottom, while the side that eventually comes into contact with air is referred to as Top.

(1.5 wt%) could have led to the formation of agglomerates, resulting in elevated peaks on the film surface and an overall increase in roughness, as indicated in Table 1. These surface irregularities are crucial to consider for subsequent deposition of transparent conductive coatings like Indium Tin Oxide (ITO). Such irregularities can lead to complications including current leakage and short-circuiting in optoelectronic devices, which could ultimately reduce the efficiency of solar cells (Kim et al., 2020) and accelerate the degradation of organic LEDs (Jonda et al., 2000).

CNF films with the lowest roughness (0.5 μm) were achieved using a 0.5 wt% concentration (Table 1). Consequently, for the next phase of our research, we deliberately chose a 0.5 wt% concentration. This decision was taken to promote the production of films with minimized roughness. This, in turn, is crucial for the effectiveness of depositing subsequent layers, while mitigating potential issues linked to device performance and longevity that were previously mentioned.

3.1.2. Impact of the grammage and pressing temperature on the film formation, roughness, and optical properties

Hereafter, by increasing the pressing temperature and the grammage of the CNF films, less transparent materials with higher values of reflectance were manufactured (Fig. 2). While the changes in pressing temperature and the grammage yielded similar results, it is important to note that the modifications within the structure were driven by distinct reasons. When the temperature increased, the removal of water from the wet film structure occurred faster. As a result of the elimination of water, the CNF films visually demonstrated a significant reduction in shape which could be attributable to the disruption of hydrogen bonds between hydroxyl groups, in agreement with the discussion presented by Zhang et al. (2017). In addition, the density of the film increased (from 1.07 g·cm^{-3} ± 0.02 to 1.25 g·cm^{-3} ± 0.02, Table 1) with the increase of the pressing temperature meaning that higher interactions in the interface of the entangled fibers could have led to a more compact material.

As expected, increasing the grammage increased the thickness of the film (from 26 μm ± 3 to 47 μm ± 2, Table 1), with no significant change in density (from 1.07 g·cm^{-3} ± 0.02 to 1.11 g·cm^{-3} ± 0.02). Consequently, the path to be traveled by the light from one side of the film to the other increased, together with the increased scattering within the material, explaining the changes in optical properties.

Regarding the haze values, the major impact was observed for the film produced using a higher pressing temperature, which could be indicative of the greater reflectance within the bulk of the film caused by its higher density (Table 1). This follows the same line of thinking when observing the minor haze change by increasing the grammage of the

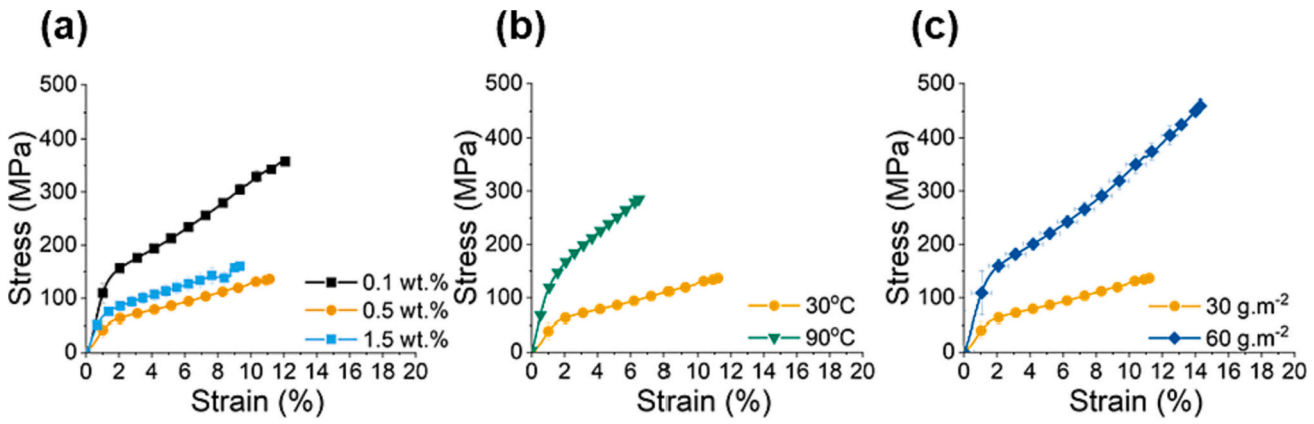

Fig. 4. Mechanical properties of CNF films. (a) Influence of the suspension concentrations, (b) the influence of the temperature in the hot press, and (c) the Influence of the grammage of the films.

Table 2
Nanocelluloses (NC) with the respective suspension concentration (Conc), grammage (Gramm), and temperature (Temp) used to produce films with different tensile strengths and young modulus.

NC	Conc (wt%)	Gramm ($g \cdot m^{-2}$)	Temp. (°C)	Tensile strength (MPa)	Young modulus (GPa)
CNF	0.1	30	30	237.1 ± 4.7	10.1 ± 0.2
	0.5			192.0 ± 11.4	9.5 ± 0.3
	1.5			152.7 ± 15.0	9.7 ± 0.1
	0.5		90	233.3 ± 4.8	12.4 ± 0.04
		60	30	196.0 ± 7.5	5.1 ± 0.7
Enz-CNF				133.5 ± 4.2	7.2 ± 0.3
CMC-CNF				173.2 ± 7.6	5.5 ± 0.9
TOCNF				187.9 ± 6.4	7.2 ± 0.95

films followed by a small variation of density (Table 1).

3.1.3. Density and roughness versus optical properties

By correlating the density and roughness of the films with their optical properties, as illustrated in Fig. 3, we observed a trend wherein denser films exhibited increased reflection and scattering of light, leading to lower transmittance. In this scenario, the elevated reflectance may be attributed, at least in part, to the backward scattering of light from the bulk of the film. Unlike density, roughness does not demonstrate a clear correlation with optical performance. As a result, these findings demonstrated that the internal structure of the film (bulk) had a greater impact on optical properties than the interfacial structure (surface).

3.1.4. Mechanical properties of CNF films

While evaluating the tensile curves of the CNF films (Fig. 4), an initial elastic deformation was observed, followed by yielding and strain hardening. The modulus observed in the elastic deformation increased considerably due to the straightening and reorientation of the cellulose fibrils in the films (Ansari & Berglund, 2016; Benítez & Walther, 2017). Then, fibers underwent displacement/slippage resulting in irreversible structural changes. Finally, the fibers aligned and consolidated into a tensile-resistant net, providing ductility to the film until break.

Hence, altering the processing variables did not affect the form of tensile test curves (Fig. 4) nor Young's modulus (Table 2); nevertheless, noticeable variations were evident in their tensile strength values (Table 2). Overall, the tensile strength was highly dependent on the density of the films (Fig. S3) meaning that the higher compaction of the fibers requires more energy for the film to break under a certain tension. In addition, the organization of the fibers in random-in-plane orientation might have a positive impact on the mechanical properties, which could explain why the films produced at a low concentration of the suspension (0.1 wt%) and low pressing temperature (30 °C), presented better mechanical properties (tensile strength: 237.1 MPa ± 4.7). Therefore, NC fibers could have greater time to organize and collapse themselves randomly, for instance when the wet film is formed from low-concentrated suspensions followed by lower pressing temperature. Lastly, increasing the grammage did not affect the density or the organization of the fibers but affected the thickness of the film (Table 1), the elongation of which requires more energy.

Overall, by changing the processing methods of a single NC grade, it was observed that factors, such as stability and homogeneity, of the initial suspensions played a crucial role in the roughness, optical, and mechanical properties of the films. The lowest concentration of CNF suspension created films with increased haze, transmittance, reflectance, strength, and roughness. By increasing the pressing temperature, the films presented lower transparency, higher reflectance, and great strength which could be attributed to the improved dryness during the pressing process. Additionally, by increasing the grammage, thicker films were produced, which impacted more significantly the optical properties and roughness than mechanical properties.

3.2. Impact of different NC grades on roughness, optical and mechanical properties

Next, we evaluated the impact of four different NC grades: CNF, Enz-CNF, TOCNF, and CMC-CNF on the overall NC film properties. These NC suspensions presented several differences, but it is important to start highlighting their functional groups. For instance, Enz-CNF and CNF do not present functional groups on their surfaces, while TOCNF and CMC-CNF carry carboxyl COOH and CH_2COOH groups, respectively (Kim et al., 2021).

As is seen in Fig. 5 - a, all the suspensions showed a gel behavior at concentrations around 2 wt%, where strong nanonetwork structures take place (the combined contribution of hydrophilicity, high specific surface area, and high CNF aspect ratio). (Heise et al., 2021; Nechyporchuk et al., 2016) Additionally, they presented different turbidity values (Fig. 5 - d), which was a consequence of the difference in nano fraction and treatments (enzymatic or chemical). For instance, carboxyl groups on CNF (TOCNF and CMC-CNF) produced fibers better dispersed in water, resulting in lower turbidity.

Initially, it was believed that the turbidity of the suspensions could be an indicative of the optical properties of the films, however, a direct relationship between the nano fraction and the transmittance/reflectance of the films was observed (Fig. 5 – b, d, e). In the case of Enz-CNF film, the lower transmittance and higher reflectance were explained by

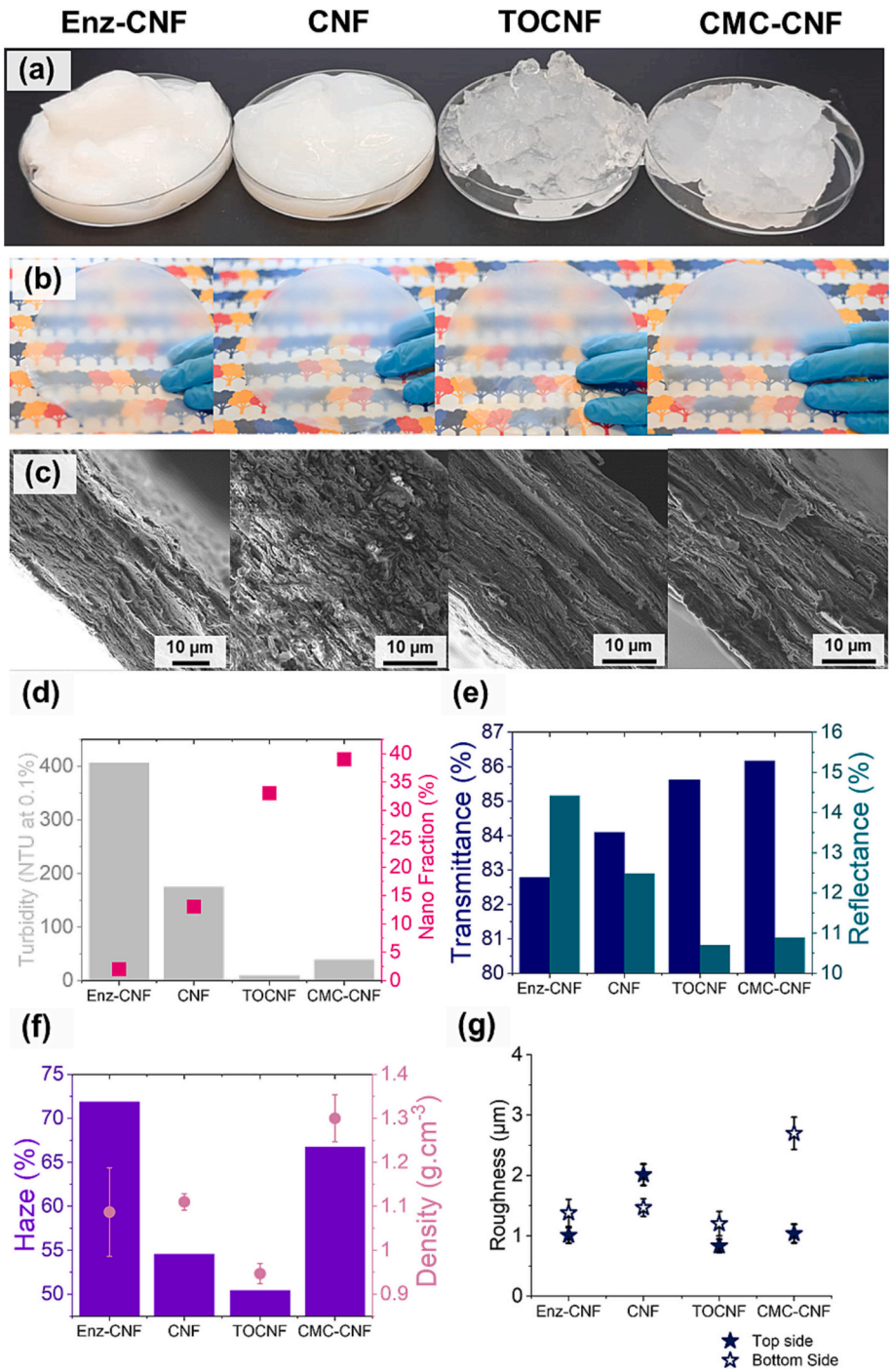

Fig. 5. (a) Different sources of CNF: Enzimared cellulose nanofibrils (Enz-CNF), Cellulose nanofibrils (CNF), TEMPO oxidized cellulose nanofibrils (TOCNF) and Carboxymethylated cellulose nanofibrils (CMC-CNF). (b) Films of Enz-CNF, CNF, TOCNF, and CMC-CNF (from the left to the right). (c) SEM image of the cross-section of the Enz-CNF, CNF, TOCNF, and CMC-CNF films (from the left to the right). (d) Turbidity and nano fraction of the suspensions (e). Transmittance and Reflectance at 550 nm, (f) correlation between haze at 550 nm and density, and (g) roughness of the films.

the low nano fraction. Thus, larger fibrils led to more voids, increasing light scattering and reducing transmittance. The more scattered light for Enz-CNF was confirmed by the haze measurement (Fig. 5 - f). However, the haze was not dependent on the nano fraction of the suspensions; instead, it correlated with the density of the films.

The SEM images (Fig. 5 – c) clearly showed differences in film structures, which led to density changes (Fig. 5 – f). All films showed laminar structures, but the CNF film showed greater fiber collapsing; in other words, the layers in the CNF film were less expressive. Both Enz-CNF and CNF presented similar values of densities, on the other hand, TOCNF and CMC-CNF had different behaviors caused by possible interference of the electrostatic charges in the film's formation. In other words, the carboxyl groups present on the surface of the NC could have interfered with the water removal and the film formation itself. In this way, as TOCNF presented higher water affinity compared to CMC-CNF, the water removal, and the film formation happened slowly inducing a denser material (Fig. 5 – f).

Regarding roughness, the films produced by the different NC grades did not present a clear relation (Fig. 5 – g). It is believed that the correlation between the initial properties of the suspensions and the

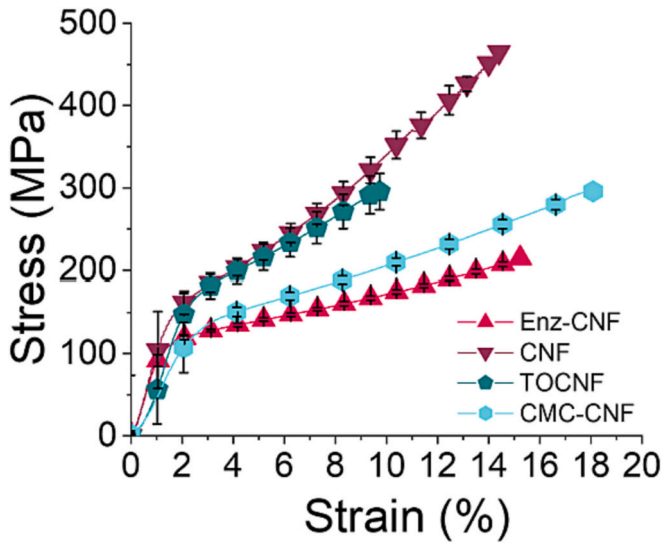

Fig. 6. Tensile curves of Enzimared cellulose nanofibrils (Enz-CNF), Cellulose nanofibrils (CNF), TEMPO-oxidized cellulose nanofibrils (TOCNF) and Carboxymethylated cellulose nanofibrils (CMC-CNF) films.

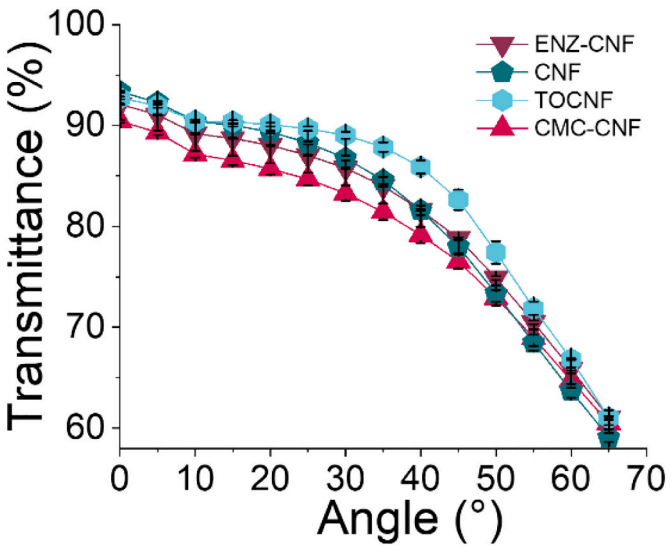

Fig. 7. Angle-dependent transmittance for ENZ-CNF, CNF, TOCNF, and CMC-CNF films, ranging from 0 to 65°. Total transmittance integrated from 500 to 900 nm.

roughness is only applied to the same NC grade. However, it was possible to observe differences between both sides of the films. The side that was in contact with the membrane (bottom) tended to have a higher roughness compared to the side of the film that was in the air (top). This can be assigned to the hypothesis of longer fibers being filtered first and being at the bottom of the film.

For quite some time, it has been established that the mechanical properties of NC films correlate with their densities (Spence et al., 2010). Specifically, denser films present higher strength and require more energy to break under a tension force. Surprisingly, in this study, it was observed that this correlation is only fair when comparing films produced by the same NC grade (Fig. 5 – f), the mechanical properties of films from different NC grades presented no correlation with their densities (Fig. 6).

Here, for the NC grades without carboxyl groups, the nano fraction content intensively affected the mechanical behavior of the films. For instance, CNF which had a higher value of nano fraction compared to Enz-CNF (Fig. 5 – d), led to stronger films (Fig. 6, Table 2). When the fibrils presented greater homogeneity in size, the compaction occurred evenly throughout the entire film, leading to greater interaction between them and requiring more energy to break the film under tension. Here, by comparing to the other NC grade films (Table 1), Enz-CNF presented a significant error in its density (Fig. 5 – f), indicating that the film was more heterogeneous and consequently also compromised the strength (Table 2).

On the other hand, the presence of carboxyl groups induced different mechanical strengths (Table 2), independently of the nano fraction of the suspensions. For instance, when comparing NC grades derived from the same cellulose source and manufactured at the same institution—Enz-CNF (133.5 ± 4.2 MPa) and CMC-CNF (173.2 ± 7.6 MPa)—the presence of carboxyl groups induced superior fibrillation in the nano fraction, thereby leading to enhanced assembly and entanglement. The same was expected for CNF (196.0 ± 7.5 MPa) and TOCNF (187.9 ± 6.4 MPa), however, the contradictory result suggests that TOCNF was highly fibrillated for a mechanical grade inducing lower mechanical properties.

Herein, it also explored the impact of different NC grades on the roughness, optical, and mechanical properties of their films. Although this investigation allows us to make adjustments in the NC films and provides important insights regarding their transparency and haze, a more comprehensive understanding of the optical properties, particularly reflectivity, is essential. Certain studies promote the utilization of NC films as substrates for the next generation of solar cells, suggesting potential benefits in terms of enhanced performance through scattering or antireflective properties. However, in our preliminary analysis, the incorporation of these CNF films as a light management layer on top of dye solar cells did not yield a statistically significant effect on the power conversion efficiency. To shed light on the underlying reasons for this phenomenon, we proceeded with an in-depth evaluation of the films of different NC grades using the angular-dependent transmittance technique. This helped to elucidate the behavior and interactions of these films with light and their feasibility in optoelectronics such as solar cells.

3.2.1. *Angular-dependent transmittance*

To measure the angular dependent transmittance, the sample was rotated to change the light incidence angle from 0° to 65° (Fig. S4) where the transmittance at 0° is comparable to the transmittance presented in Fig. 5 – e (measured at different device). All NC films presented transmittance between 90 and 95 % at 0° (Fig. 7), which noticeably decreased at angles >30°. Overall, the transmittance decreased between 0° and 65° (Fig. 7). The transmittance loss at high angles suggests that the light scattering is not entirely directed forward and that some light is reflected.

Comparable loss in transmittance at angles higher than 40° was not observed for standard optoelectronic substrate materials, glass, PET, and PEN (Fig. S5). A high transmittance is critical because it is directly proportional to the number of light interactions within the active layer of the photoelectronic. For instance, in solar cells, the decrease in the substrate transparency negatively affects the photocurrent produced by the device. Furthermore, most solar devices are stationary, meaning that light will enter the device at an angle, which is why it is important that light can pass through at a wide range of angles.

Fang et al. reported a noticeable increase in the photocurrent (over 15 %) as compared to a conventional cell without a light management layer, specifically at high incident angles (between 60 and 87°) for an organic solar cell with TOCNF film glued on its glass surface (Fang et al., 2014). The authors described the improved light absorption of the active layer as a consequence of a longer light path length across the active area due to an increased forward light scattering in the NC film (high haze). However, both our samples and the samples investigated by Fang et al. have high transmission haze (between 50 and 70 % for our samples and ~60 % for Fang et al.). Thus, high haze does not automatically correlate to an increased optical performance. This difference in optics could be

Table 3
Tensile strength (MPa), Transmittance (%), Haze (%), and Roughness (nm) of different cellulose films used to produce optoelectronic applications with different performances.

Cellulose film	Optoelectronics	Tensile strength (MPa)	Transmittance (%)	Haze (%)	Roughness (nm)	Ref.
Regular paper and carboxymethylated cellulose composite	Perovskite solar cells*	~36	90.1£	95.2£	–	(Hou et al., 2020)
TOCNF	Polycrystalline silicon solar cells*	~93	90.2£	46.5£	–	(Chen et al., 2018)
TOCNF	Organic light-emitting diodes#	287	~90£	~50£	7.7	(Zhu et al., 2013)
Acrylic-coated NC paper	Perovskite solar cells#	81	91.71£	–	2.15	(Gao et al., 2019)
TOCNF/Ag NWs composite	Organic solar cells#	70.1	~75£	–	28	(Lin et al., 2021)
Regenerated cellulose	Electrodes#	110	~75£	–	–	(Tao et al., 2020)
Decolorated lignocellulosic nano paper	Gallium arsenide solar cells*	105	90	46£	4.4 ± 0.6	(Jiang et al., 2020)
Composite paper from O-(2,3-Dihydroxypropyl) cellulose and tunicate cellulose nanocrystals	Polymer solar cells#	~15	85	–	–	(Cheng et al., 2018)
TOCNF composite with conductive polymerizable deep eutectic solvent	Electroluminescent#	~33	94.5£	–	–	(Zhang et al., 2020)
CNF - 0.1 wt. 30 °C 30 g·m^{-2}	–	237 ± 5	86.1£	55.5£	1.5 ± 0.2$^{\eta1}$ 1.3 ± 0.2$^{\eta2}$	our study

* Light management, # Substrates, £ Wavelength at 550 nm, β enhancement of performance compared to bare device, σ power conversion efficiency, η1 Roughness bottom side (μm), η2 Roughness top side (μm).

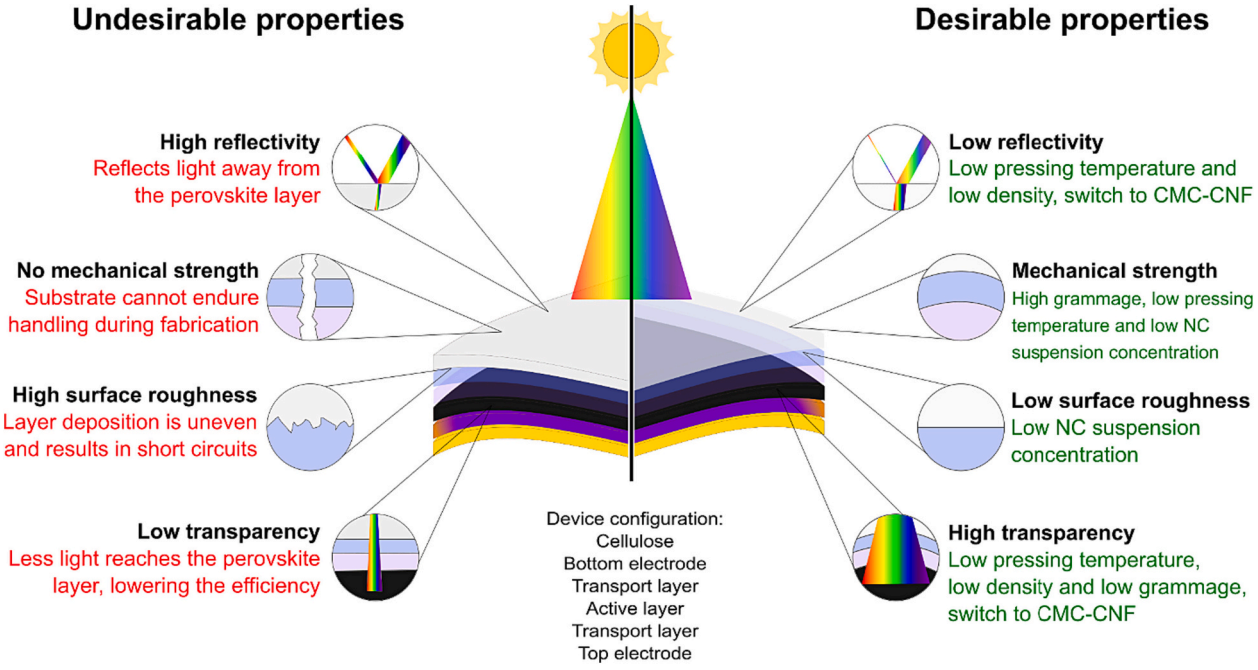

Fig. 8. Schematic of a standard optoelectronic cellulosic device with undesirable and desirable properties.

related to the different microstructure and/or porosity of the films caused by the production of films using different NC grades. In addition, TOCNF films have been shown as prospective antireflective materials (Azzam et al., 2014) where the antireflection properties could be manipulated by engineering the porosity of the films, thus changing the refractive index. Unfortunately, we could not compare our results with those found in the literature for antireflection application, since it was reported only at 0° incidence angle. (Azzam et al., 2014) We suggest that engineering the index of refraction should be prioritized, and detailed attention to scattering direction at all incidence angles is needed with high haze.

3.3. Suitability of NC films as substrates for optoelectronics

Up to this point, we have showcased how NC films can be easily modified to produce substrates for tentative use in optoelectronics. However, while these materials offer adaptability, they might not represent the optimal choice for nature-inspired flexible devices, since they would still require better surface qualities (lower roughness), lower energy consumption of the extraction process, and production up-scaling (Suresh Khurd & Kandasubramanian, 2022). The advantages of employing NC in optoelectronics extend beyond its renewability. It enables the rapid production of electronics through efficient roll-to-roll processes, to a vast range of fabrication methods, which contribute not only to the materials' properties but to the performance of the

optoelectronics produced (Table 3).

The efficiency of the final optoelectronic device builds on low surface roughness, high transmittance, low reflectance, and sufficient mechanical strength of the substrate, as illustrated in Fig. 8. The low roughness of a substrate ensures the uniformity of all the layers deposited on its surface. This quality is crucial for the fabrication of optoelectronic devices. In contrast, a rough electrode not only lowers conductivity and optical properties but if the peaks on its surface are too tall, there is a risk that they penetrate other functional layers and short-circuit the whole device (Bragaglia et al., 2019). In our study, we obtained a lower roughness by altering the NC suspension concentration, but when we compared it with previous studies (Table 3) we could see clearly that our results were below the benchmark for an optimal roughness.

In optoelectronics, transparency, and reflectivity of a substrate play crucial roles in determining their performance and quality. The NC films produced here presented overall high transparency improved by low concentrations and highly fibrillated NC grades, but in all, transmittance was comparable to those found in Table 3. Furthermore, our study on angular-dependent transmittance showed that, while films have good transmittance with direct irradiation, they present high reflectance at high incidence angles, which is an undesirable quality for optoelectronic devices that depend on incoming light, like solar cells and light sensors. Films with different levels of haze displayed similar angular-dependent transmittance curves, showing how there is not a direct relation between haze and antireflectiveness. Lastly, flexible optoelectronics require enough mechanical strength to endure stress during the fabrication process. NC films produced in this study presented mechanical properties comparable to those found in the literature (Table 3) and were suitable to act as substrates for solar cells, LEDs, and other optoelectronic devices when considering this perspective.

4. Conclusions

This research provided compelling evidence supporting the central hypothesis that making simple adjustments to processing factors and manipulating CNF suspension properties can indeed lead to significant changes in the surface (roughness), and optical and mechanical properties of CNF films.

First and foremost, it was demonstrated that the homogeneity and colloidal stability of CNF suspensions were pivotal factors in film formation. Stable suspensions with strong interconnections among nanofibrils yielded films with lower roughness, making them suitable for applications requiring efficient layer deposition. Conversely, less stable suspensions lead to inhomogeneous films with higher roughness, which can be problematic for devices like solar cells and optoelectronics.

Furthermore, the impact of different NC grades (unmodified fibrillated CNF, enzymatic CNF, TEMPO-oxidized CNF, and carboxymethylated CNF) on film properties was investigated, revealing that the nano fraction of the NC suspensions plays a critical role in determining both optical and mechanical characteristics. Our study highlights the need for careful selection of NC grades to meet specific application requirements.

Considering these findings, it is evident that by tailoring processing parameters and choosing the right NC grade, it is possible to achieve CNF films with precisely tuned optical and mechanical properties. However, it is still necessary to overcome issues related to how rough the surface is and external interactions, such as water absorption and swelling. Nevertheless, the ability to optimize CNF film properties through simple adjustments opens new avenues for the development of high-performance materials in various technological fields.

CRediT authorship contribution statement

Joice Jaqueline Kaschuk: Writing – review & editing, Writing – original draft, Visualization, Project administration, Methodology, Investigation, Formal analysis, Data curation, Conceptualization. **Yazan Al Haj:** Writing – review & editing, Investigation, Data curation. **Joaquin Valdez Garcia:** Writing – review & editing, Writing – original draft, Validation, Investigation, Formal analysis, Data curation. **Aleksi Kamppinen:** Writing – review & editing, Formal analysis, Data curation. **Orlando J. Rojas:** Writing – review & editing, Supervision, Resources, Funding acquisition. **Tiffany Abitbol:** Writing – review & editing, Visualization, Supervision, Conceptualization. **Kati Miettunen:** Writing – review & editing, Visualization, Supervision, Resources, Funding acquisition, Conceptualization. **Jaana Vapaavuori:** Writing – review & editing, Supervision, Resources, Project administration, Funding acquisition, Conceptualization.

Declaration of competing interest

The authors declare the following financial interests/personal relationships which may be considered as potential competing interests: Jaana Vapaavuori reports financial support was provided by Academy of Finland. Joice Jaqueline Kaschuk reports financial support was provided by Academy of Finland. Tiffany Abitbol reports financial support was provided by Swedish Research Council Formas. Yazan Al Haj reports financial support was provided by Academy of Finland. Joaquin Valdez Garcia reports financial support was provided by Academy of Finland. Aleksi Kamppinen reports financial support was provided by Academy of Finland. Orlando J Rojas reports financial support was provided by European Research Council.

Data availability

Data will be made available on request.

Acknowledgements

This work was a part of the Academy of Finland's Flagship Programme under Projects No. 318890 and 318891 (Competence Center for Materials Bioeconomy, FinnCERES). J.V. acknowledges the Academy of Finland project "SUBSTAINABLE" (Decision number 334818) for generous funding. T.A. acknowledges funding from Formas for the "SUBSTAINABLE" project granted through the Tandem Forest Values program (Formas grant number 2019–02508). J. V. G acknowledges funding from Academy of Finland (Bio-EST, 336441) and Finnish Cultural Foundation. A. K. acknowledges funding from: UTUGS graduate school. K. M. acknowledges the Academy of Finland project Bio-EST, 336577. O.J.R. and J.J.K. acknowledge funding support from the European Research Council (ERC) under the European Union's Horizon 2020 research and innovation program (grant agreement No 788489, "BioElCell"). We also thank Mr. Tommi Harju for the preparation of the optical setup for the angle-dependent transmittance measurements.

Appendix A. Supplementary data

Supplementary data to this article can be found online at https://doi.org/10.1016/j.carbpol.2024.121877.

References

Ahankari, S. S., Subhedar, A. R., Bhadauria, S. S., & Dufresne, A. (2021). Nanocellulose in food packaging: A review. *Carbohydrate Polymers, 255*, Article 117479. https://doi.org/10.1016/j.carbpol.2020.117479

Ajdary, R., Huan, S., Zanjanizadeh Ezazi, N., et al. (2019). Acetylated nanocellulose for single-component bioinks and cell proliferation on 3D-printed scaffolds. *Biomacromolecules, 20*, 2770–2778. https://doi.org/10.1021/acs.biomac.9b00527

Ansari, F., & Berglund, L. A. (2016). Tensile properties of wood cellulose nanopaper and nanocomposite films. In *Multifunctional polymeric nanocomposites based on cellulosic reinforcements* (pp. 115–130). Elsevier.

Azzam, F., Moreau, C., Cousin, F., et al. (2014). Cellulose nanofibril-based multilayered thin films: Effect of ionic strength on porosity, swelling, and optical properties. *Langmuir, 30*, 8091–8100. https://doi.org/10.1021/la501408r

Benítez, A. J., & Walther, A. (2017). Cellulose nanofibril nanopapers and bioinspired nanocomposites: A review to understand the mechanical property space. *Journal of*

Materials Chemistry A Materials, 5, 16003–16024. https://doi.org/10.1039/C7TA02006F
Bragaglia, M., Lamastra, F. R., Tului, M., et al. (2019). Low temperature sputtered ITO on glass and epoxy resin substrates: Influence of process parameters and substrate roughness on morphological and electrical properties. *Surfaces and Interfaces, 17*, Article 100365. https://doi.org/10.1016/j.surfin.2019.100365
Chattopadhyay, S., & Labram, J. G. (2022). The effect of substrate curvature on capacitance and transfer characteristics for thin film transistors on the surface of spheres. *Journal of Applied Physics, 132*. https://doi.org/10.1063/5.0118236
Chen, F., Xiang, W., Sawada, D., et al. (2020). Exploring large ductility in cellulose nanopaper combining high toughness and strength. *ACS Nano, 14*, 11150–11159. https://doi.org/10.1021/acsnano.0c02302
Chen, S., Song, Y., & Xu, F. (2018). Highly transparent and hazy cellulose nanopaper simultaneously with a self-cleaning superhydrophobic surface. *ACS Sustainable Chemistry & Engineering, 6*, 5173–5181. https://doi.org/10.1021/acssuschemeng.7b04814
Chen, Y., Zhang, L., Yang, Y., et al. (2021). Recent progress on nanocellulose aerogels: preparation, modification, composite fabrication. *Applications. Advanced Materials, 33*. https://doi.org/10.1002/adma.202005569
Cheng, Q., Ye, D., Yang, W., et al. (2018). Construction of transparent cellulose-based nanocomposite papers and potential application in flexible solar cells. *ACS Sustainable Chemistry & Engineering, 6*, 8040–8047. https://doi.org/10.1021/acssuschemeng.8b01599
Deepa, B., Abraham, E., Cordeiro, N., et al. (2015). Utilization of various lignocellulosic biomass for the production of nanocellulose: A comparative study. *Cellulose, 22*, 1075–1090. https://doi.org/10.1007/s10570-015-0554-x
Dufresne, A. (2013). Nanocellulose: A new ageless bionanomaterial. *Materials Today, 16*, 220–227. https://doi.org/10.1016/j.mattod.2013.06.004
Fang, Z., Zhu, H., Yuan, Y., et al. (2014). Novel nanostructured paper with ultrahigh transparency and ultrahigh haze for solar cells. *Nano Letters, 14*, 765–773. https://doi.org/10.1021/nl404101p
Fukuzumi, H., Saito, T., Iwata, T., et al. (2009). Transparent and high gas barrier films of cellulose nanofibers prepared by TEMPO-mediated oxidation. *Biomacromolecules, 10*, 162–165. https://doi.org/10.1021/bm801065u
Gao, L., Chao, L., Hou, M., et al. (2019). Flexible, transparent nanocellulose paper-based perovskite solar cells. *npj Flexible Electronics, 3*, 4. https://doi.org/10.1038/s41528-019-0048-2
Hancock, J., Osei-Bonsu, R., Hoque, M., et al. (2023). Valorization of cannabis green waste to cellulose nanomaterials via phosphoric acid hydrolysis. *Industrial Crops and Products, 201*, Article 116888. https://doi.org/10.1016/J.INDCROP.2023.116888
Haron, G. A. S., Mahmood, H., Noh, M. H., et al. (2021). Ionic liquids as a sustainable platform for nanocellulose processing from bioresources: Overview and current status. *ACS Sustainable Chemistry & Engineering, 9*, 1008–1034. https://doi.org/10.1021/acssuschemeng.0c06409
Heise, K., Kontturi, E., Allahverdiyeva, Y., et al. (2021). Nanocellulose: Recent fundamental advances and emerging biological and biomimicking applications. *Advanced Materials, 33*, Article 2004349. https://doi.org/10.1002/adma.202004349
Henriksson, M., Berglund, L. A., Isaksson, P., et al. (2008). Cellulose nanopaper structures of high toughness. *Biomacromolecules, 9*, 1579–1585. https://doi.org/10.1021/bm800038n
Hou, G., Liu, Y., Zhang, D., et al. (2020). Approaching theoretical haze of highly transparent all-cellulose composite films. *ACS Applied Materials & Interfaces, 12*, 31998–32005. https://doi.org/10.1021/acsami.0c08586
Jacucci, G., Schertel, L., Zhang, Y., et al. (2020). Light management with natural materials: From whiteness to transparency. *Advanced Materials*. , Article 2001215. https://doi.org/10.1002/adma.202001215
Jia, C., Li, T., Chen, C., et al. (2017). Scalable, anisotropic transparent paper directly from wood for light management in solar cells. *Nano Energy, 36*, 366–373. https://doi.org/10.1016/j.nanoen.2017.04.059
Jiang, Y., Wang, Z., Liu, X., et al. (2020). Highly transparent, UV-shielding, and water-resistant lignocellulose nanopaper from agro-industrial waste for green optoelectronics. *ACS Sustainable Chemistry & Engineering, 8*, 17508–17519. https://doi.org/10.1021/acssuschemeng.0c06752
Jonda, C., Mayer, A. B. R., Stolz, U., et al. (2000). Surface roughness effects and their influence on the degradation of organic light emitting devices. *Journal of Materials Science, 35*, 5645–5651. https://doi.org/10.1023/A:1004842004640/METRICS
Kaschuk, J. J., Al Haj, Y., Rojas, O. J., et al. (2021). Plant-based structures as an opportunity to engineer optical functions in next-generation light management. *Advanced Materials, 34*, Article 2104473. https://doi.org/10.1002/adma.202104473
Kaschuk, J. J., Al Haj, Y., Rojas, O. J., et al. (2022). Plant-based structures as an opportunity to engineer optical functions in next-generation light management. *Advanced Materials, 34*, Article 2104473. https://doi.org/10.1002/adma.202104473
Kim, H. J., Roy, S., & Rhim, J. W. (2021). Effects of various types of cellulose nanofibers on the physical properties of the CNF-based films. *Journal of Environmental Chemical Engineering, 9*, Article 106043. https://doi.org/10.1016/J.JECE.2021.106043
Kim, S. H., Oh, Y.-J., & Lee, D. Y. (2020). Influence of surface roughness on the efficiency of a flexible organic solar cell. *Journal of Ceramic Processing Research, 21*, 42–49. https://doi.org/10.36410/jcpr.2020.21.1.42
Koga, H., & Nogi, M. (2015). Flexible paper electronics. In *Organic electronics materials and devices* (pp. 101–115). Tokyo: Springer Japan.
Lengowski, E. C., Franco, T. S., Viana, L. C., et al. (2023). Micro and nanoengineered structures and compounds: Nanocellulose. *Cellulose*. https://doi.org/10.1007/s10570-023-05532-x
Lin, P.-C., Hsieh, C.-T., Liu, X., et al. (2021). Fabricating efficient flexible organic photovoltaics using an eco-friendly cellulose nanofibers/silver nanowires conductive substrate. *Chemical Engineering Journal, 405*, Article 126996. https://doi.org/10.1016/j.cej.2020.126996
Liu, W., Liu, K., Du, H., et al. (2022). Cellulose nanopaper: Fabrication, functionalization, and applications. *Nanomicro Letters, 14*, 1–27. https://doi.org/10.1007/s40820-022-00849-x
Nechyporchuk, O., Belgacem, M. N., & Pignon, F. (2016). Current progress in rheology of cellulose nanofibril suspensions. *Biomacromolecules, 17*, 2311–2320. https://doi.org/10.1021/acs.biomac.6b00668
Niinivaara, E., & Cranston, E. D. (2020). Bottom-up assembly of nanocellulose structures. *Carbohydrate Polymers, 247*, Article 116664. https://doi.org/10.1016/j.carbpol.2020.116664
Pires, J. R. A., Souza, V. G. L., & Fernando, A. L. (2019). Valorization of energy crops as a source for nanocellulose production – Current knowledge and future prospects. *Industrial Crops and Products, 140*, Article 111642. https://doi.org/10.1016/j.indcrop.2019.111642
Podsiadlo, P., Sui, L., Elkasabi, Y., et al. (2007). Layer-by-layer assembled films of cellulose nanowires with antireflective properties. *Langmuir, 23*, 7901–7906. https://doi.org/10.1021/la700772a
Pradhan, D., Jaiswal, A. K., & Jaiswal, S. (2022). Emerging technologies for the production of nanocellulose from lignocellulosic biomass. *Carbohydrate Polymers, 285*, Article 119258. https://doi.org/10.1016/j.carbpol.2022.119258
Qing, Y., Sabo, R., Wu, Y., et al. (2015). Self-assembled optically transparent cellulose nanofibril films: Effect of nanofibril morphology and drying procedure. *Cellulose, 22*, 1091–1102. https://doi.org/10.1007/s10570-015-0563-9
Rol, F., Vergnes, B., El Kissi, N., & Bras, J. (2020). Nanocellulose production by twin-screw extrusion: Simulation of the screw profile to increase the productivity. *ACS Sustainable Chemistry & Engineering, 8*, 50–59. https://doi.org/10.1021/acssuschemeng.9b01913
Saito, T., Kimura, S., Nishiyama, Y., & Isogai, A. (2007). Cellulose Nanofibers Prepared by TEMPO-Mediated Oxidation of Native Cellulose. *Biomacromolecules, 8*(8), 2485–2491. https://doi.org/10.1021/bm0703970
Shanmugam, K., Nadeem, H., Browne, C., et al. (2020). Engineering surface roughness of nanocellulose film via spraying to produce smooth substrates. *Colloids and Surfaces A: Physicochemical and Engineering Aspects, 589*, Article 124396. https://doi.org/10.1016/j.colsurfa.2019.124396
Solhi, L., Guccini, V., Heise, K., et al. (2023). Understanding nanocellulose-water interactions: Turning a detriment into an asset. *Chemical Reviews, 123*, 1925–2015.
Spence, K. L., Venditti, R. A., Habibi, Y., et al. (2010). The effect of chemical composition on microfibrillar cellulose films from wood pulps: Mechanical processing and physical properties. *Bioresource Technology, 101*, 5961–5968. https://doi.org/10.1016/j.biortech.2010.02.104
Squinca, P., Bilatto, S., Badino, A. C., & Farinas, C. S. (2020). Nanocellulose production in future biorefineries: An integrated approach using tailor-made enzymes. *ACS Sustainable Chemistry & Engineering, 8*, 2277–2286. https://doi.org/10.1021/acssuschemeng.9b06790
Suresh Khurd, A., & Kandasubramanian, B. (2022). A systematic review of cellulosic material for green electronics devices. *Carbohydrate Polymer Technologies and Applications, 4*, Article 100234. https://doi.org/10.1016/j.carpta.2022.100234
Tao, T., Liu, X., Islam, A., et al. (2020). Flexible and conductive cellulose substrate by layered growth of silver nanowires and indium-doped tin oxide. *Bioresources, 15*, 4699–4710. https://doi.org/10.15376/biores.15.3.4699-4710
Wang, Y., & Huang, J.-T. (2021). Transparent, conductive and superhydrophobic cellulose films for flexible electrode application. *RSC Advances, 11*, 36607–36616. https://doi.org/10.1039/D1RA06865B
Yang, H., Jacucci, G., Schertel, L., & Vignolini, S. (2022). Cellulose-based scattering enhancers for light management applications. *ACS Nano, 16*, 7373–7379. https://doi.org/10.1021/acsnano.1c09198
Yang, T., Li, X., Guo, Y., et al. (2023). Preparation of nanocellulose crystal from bleached pulp with an engineering cellulase and co-production of ethanol. *Carbohydrate Polymers, 301*, Article 120291. https://doi.org/10.1016/j.carbpol.2022.120291
Yang, W., Jiao, L., Liu, W., et al. (2018). Morphology control for tunable optical properties of cellulose nanofibrils films. *Cellulose, 25*, 5909–5918. https://doi.org/10.1007/s10570-018-1974-1
Zhang, K., Chen, G., Li, R., et al. (2020). Facile preparation of highly transparent conducting nanopaper with electrical robustness. *ACS Sustainable Chemistry & Engineering, 8*, 5132–5139. https://doi.org/10.1021/acssuschemeng.9b07266
Zhang, X.-F., Feng, Y., Huang, C., et al. (2017). Temperature-induced formation of cellulose nanofiber film with remarkably high gas separation performance. *Cellulose, 24*, 5649–5656. https://doi.org/10.1007/s10570-017-1529-x
Zhang, Y., Zhang, L., Cui, K., et al. (2018). Flexible electronics based on micro/nanostructured paper. *Advanced Materials, 30*, 1801588. https://doi.org/10.1002/adma.201801588
Zhao, Y., Moser, C., Lindström, M. E., et al. (2017). Cellulose nanofibers from softwood, hardwood, and tunicate: Preparation–structure–film performance interrelation. *ACS Applied Materials & Interfaces, 9*, 13508–13519. https://doi.org/10.1021/acsami.7b01738
Zhu, H., Fang, Z., Preston, C., et al. (2014). Transparent paper: Fabrications, properties, and device applications. *Energy & Environmental Science, 7*, 269–287. https://doi.org/10.1039/C3EE43024C
Zhu, H., Xiao, Z., Liu, D., et al. (2013). Biodegradable transparent substrates for flexible organic-light-emitting diodes. *Energy & Environmental Science, 6*, 2105. https://doi.org/10.1039/c3ee40492g